

1 Revision 1

2 **A systematic assessment of the diamond trap method for measuring fluid**
3 **compositions in high-pressure experiments**

4
5 **GRETA RUSTIONI, ANDREAS AUDÉTAT, AND HANS KEPPLER**

6 Bayerisches Geoinstitut, Universität Bayreuth, 95440 Bayreuth, Germany

7
8 **ABSTRACT**

9 A variety of experimental techniques have been proposed to measure the composition of aqueous fluids in
10 high-pressure experiments. In particular, the “diamond trap method”, where the fluid is sampled in the
11 pore space of diamond powder and analyzed by laser-ablation ICP-MS after the experiment, has become a
12 popular tool. Here, we carried out several tests in order to assess the reliability of this method. (i) We
13 prepared several capsules loaded with fluid of known composition and analyzed the fluid by laser-
14 ablation ICP-MS, either (a) after drying the diamond trap at ambient condition, (b) after freezing and
15 subsequent freeze-drying, and (c) after freezing and by analyzing a frozen state. Of these methods, the
16 analysis in the frozen state (c) was most accurate, while the results from the other two methods were
17 poorly reproducible and the averages sometimes deviated from the expected composition by more than a
18 factor of 2. (ii) We tested the reliability of the diamond trap method by using it to measure mineral
19 solubilities in some well-studied systems at high pressure and high temperature in piston cylinder runs. In
20 the systems quartz-H₂O, forsterite-enstatite-H₂O, and albite-H₂O, the results from analyzing the diamond
21 trap in frozen state by laser-ablation ICP-MS generally agreed well with the expected compositions
22 according to literature data. However, in the systems corundum-H₂O and rutile-H₂O, the data from the

23 analysis of the diamond trap were poorly reproducible and appeared to indicate much higher solubilities
24 than expected. We attribute this not to some unreliability of the analytical method, but rather to the fact
25 that in these systems, minor temperature gradients along the capsule may induce the dissolution and re-
26 precipitation of material during the run, which causes a contamination of the diamond trap by solid
27 phases. (iii) We carried out several tests on the reliability of the diamond trap to measure fluid
28 compositions and trace element partition coefficients in the eclogite-fluid system at 4 GPa and 800 °C
29 using piston cylinder experiments. The good agreement between “forward” and “reversed” experiments –
30 with trace elements initially either doped in the solid starting material or the fluid – as well as the
31 independence of partition coefficients on bulk concentrations suggests that the data obtained are reliable
32 in most cases. We also show that the rate of quenching/cooling has little effect on the analytical results,
33 that temperature oscillations during the run can be used to enhance grain growth, and that well
34 equilibrated samples can be obtained in conventional piston cylinder runs. Overall, our results suggest
35 that the diamond trap method combined with laser-ablation ICP-MS in frozen state yields reliable results
36 accurate within a factor of two in most cases; however, the precipitation of accessory minerals in the
37 diamond trap during the run may severely affect the data in some systems and may lead to a gross
38 overestimation of fluid concentrations.

39 **Keywords:** Fluids, diamond trap, high-pressure experiments, laser-ablation ICP-MS, solubility,
40 fluid/mineral partitioning

41

42

INTRODUCTION

43 Aqueous fluids are important agents of metasomatism in Earth’s mantle, particularly above subduction
44 zones (e.g. Tatsumi 1989, Manning 2004, Kelley and Cottrell 2009, Keppler 2017). Traces of such fluids
45 are sometimes sampled as fluid inclusions in mantle xenoliths and in diamonds (e.g. Kawamoto et al.
46 2013, Weiss et al. 2015). However, in particular the fluids sampled by diamonds may be the result of

47 extensive fractionation processes, which are not easy to unravel. Constraining the primary composition of
48 mantle fluids therefore requires experimental studies. Unfortunately, methods for the direct withdrawal
49 and analysis of fluids are limited to very low pressures (Potter et al. 1987) and cannot be used under
50 typical mantle P, T conditions. Simply quenching fluids equilibrated with minerals at high P and T and
51 analyzing the quenched fluid at ambient conditions is not likely to yield meaningful results, because in
52 most cases, solutes will precipitate as solid phases even during rapid quenching (e.g. Ryabchikov and
53 Boettcher 1980). Various methods have been proposed to solve this problem. In simple systems, where
54 minerals dissolve congruently, the weight loss of single crystals may allow very accurate solubility
55 measurements, since during quenching, solute will precipitate throughout the fluid, and only a very minor
56 fraction could produce an overgrowth on the original single crystal (e.g. Manning 1994, Tropper and
57 Manning 2007). Separating the charge into different, but connected compartments for solid phases and
58 fluid – by using a double capsule technique (Anderson and Burnham 1965) or folded capsules
59 (Ryabchikov and Boettcher 1980) – may also help to distinguish material precipitated from the fluid from
60 solids that were stable during run conditions.

61 Synthetic fluid inclusions offer an attractive possibility to trap fluids in high-pressure experiments. The
62 fluid inclusions may be analyzed at ambient conditions by laser-ablation ICP-MS or other methods, such
63 as synchrotron X-ray fluorescence. This technique has been used successfully to study fluid compositions
64 in various systems (Bali et al. 2011, 2012, Tsay et al. 2014). One limitation of the method is that elements
65 contained in the host crystal (typically quartz or olivine) obviously cannot be quantified. Moreover, it is
66 not always possible to accurately control the time at which the inclusions seal off and lose contact to the
67 main fluid reservoir. In systems where chemical equilibrium is attained slowly, this may have the effect
68 that the fluid trapped in the inclusions has not yet fully equilibrated with the other phases present.

69 Direct observation of mineral dissolution in the externally-heated diamond anvil cell can provide accurate
70 solubility data for minerals that dissolve congruently in the fluid (e.g. Audétat and Keppler 2005, Bernini
71 et al. 2013), but the approach does not allow to determine the solubility of minerals that dissolve

72 incongruently. Solubility studies may also be carried out by directly measuring fluid compositions in-situ
73 by X-ray fluorescence or X-ray absorption spectroscopy (e.g. Wilke et al. 2012). Other spectroscopic
74 methods, in particular Raman spectroscopy, may also be used to infer solute concentrations. However,
75 Raman spectroscopic measurements in the diamond cell require an extremely careful calibration (see
76 Zarei et al. 2018 for discussion). A general limitation of solubility studies in the externally-heated
77 diamond cell is that run durations are usually relatively short, such that systems that require long
78 timescales (more than a few hours) for equilibration cannot be studied. Moreover, controlling oxygen
79 fugacity in the diamond cell is nearly impossible.

80 The “diamond trap method” for measuring fluid (and melt) compositions was first introduced by
81 Ryabchikov et al. (1989). It may be used in conventional piston cylinder or multi anvil experiments. A
82 layer of diamond powder is placed together with the other starting materials inside a noble metal capsule.
83 During the experiment, the fluid infiltrates the pore space between the diamond grains. Upon quenching,
84 any material precipitating from the fluid will remain trapped between the diamond grains. Therefore,
85 ideally, it should be possible to determine the original bulk composition of the fluid by analyzing the
86 entire diamond trap containing the precipitated material together with the residual fluid. Since its first
87 description, the diamond trap method has been used extensively to infer fluid or melt compositions. For
88 analyzing aqueous fluids, in earlier studies (e.g. Stalder et al. 1998, Johnson and Plank 1999) the water
89 was simply allowed to evaporate after opening the capsule and the remaining solid residue was analyzed.
90 Kessel et al. (2004) introduced a more advanced method, where the capsule is first frozen and then cut
91 open and analyzed in frozen state.

92 Even though the diamond trap method – in various variants (e.g. Stalder et al. 1998, Johnson and Plank
93 1999, Kessel et al. 2005a, Rustioni et al. 2019) – has become rather popular for determining fluid
94 compositions, the accuracy and precision of this method have been evaluated only for a single
95 measurement of quartz solubility in water (Aerts et al. 2010). In this study, we therefore carried out
96 additional tests to verify the reliability of the diamond trap technique: (i) We loaded capsules containing

97 diamond traps with fluids of known composition and analyzed them by laser-ablation ICP-MS, either
98 after simple evaporation of H₂O, after freeze-drying, or in frozen state; (ii) we used the diamond trap
99 technique to measure mineral solubilities at high pressure and temperature in several simple systems,
100 where independent, high-quality solubility data exist; and (iii) we used the method to determine fluid
101 compositions and fluid/mineral partition coefficients of trace elements in the eclogite-H₂O±NaCl system.
102 In the latter experiments, we tested the attainment of equilibrium by forward and reverse experiments and
103 we investigated the effect of various experimental parameters, such as cooling or quench rates on the
104 analytical results.

105

106

EXPERIMENTAL METHODS

107 **Starting materials**

108 Several solid starting materials and solutions were prepared in order to test different aspects of the
109 diamond trap technique. Solubility measurements were carried out for quartz, forsterite-enstatite,
110 corundum, rutile and albite in water. The quartz was a very pure synthetic crystal from China (< 20 ppm
111 total impurities). Natural, inclusion-free forsterite-rich olivine (Fo₉₀) from San Carlos with a composition
112 similar to that used by Newton and Manning (2002), and enstatite (En₈₉Fs₀₉Wo₀₂Ac₀₀) from a metasomatic
113 vein in equilibrium with the peridotite also from San Carlos, were used for the forsterite-enstatite-water
114 system. For corundum, we selected a synthetic, optical sapphire crystal that is very pure according to
115 Laser-Ablation Inductively-Coupled-Plasma Mass-Spectrometry (LA-ICP-MS) analyses (only
116 measurable impurity 2600 ppm Si). Rutile was also a very pure synthetic crystal (main impurity up to 800
117 ppm Al). For albite, a natural inclusion-free crystal from Brazil, containing only 0.2 wt% K₂O and <0.05
118 wt% CaO, was selected. All the different crystals were crushed into fine powders, and for the forsterite-
119 enstatite experiment, a mixture consisting of 15 wt. % olivine and 85 wt. % enstatite was prepared.

120 For partitioning experiments in the eclogite-water system, we used a K-free synthetic basalt with a
121 composition similar to the starting material of Kessel et al. (2005a) to reproduce an average mid ocean
122 ridge basalt (MORB). SiO₂, TiO₂, Al(OH)₃, Fe₂O₃, Mg(OH)₂, CaCO₃ and Na₂CO₃ were ground and mixed
123 in an agate mortar under ethanol. The mixture was decarbonated in a Pt crucible at 1100 °C for 12 hours.
124 After cooling, the material was melted at 1600 °C for 80 minutes and quenched in distilled water to
125 prevent crystallization. The recovered glass was ground to a powder except for three pieces from different
126 portions of the crucible that were analyzed by LA-ICP-MS to assess the final composition and
127 homogeneity of the obtained starting material. In order to dope the trace elements into the MORB starting
128 material, two diopside composition glasses with different concentration of trace elements were
129 synthesized. To produce these doped diopside glasses, a procedure similar to that described above for the
130 MORB was used. In the forward experiments, the basaltic starting material was mixed with 0.4, 1 or 2 wt.
131 % of doped diopside glass in order to achieve different trace element concentrations. Circa 1 wt. % of
132 natural garnet seeds from Grytting (Norway) eclogite was also added to enhance garnet growth during the
133 experiments.

134 Saline aqueous solutions were used in some of the eclogite-fluid partitioning experiments. NaCl was
135 directly added to distilled water to obtain 1, 5, 10 and 15 wt. % NaCl solutions. Also, in order to perform
136 reversed experiments, two trace element-doped solutions were prepared by mixing appropriate amounts
137 of ICP-MS calibration solution (containing 1000 ppm of each trace element in 5 % HNO₃). The resulting
138 solution was evaporated under an infrared lamp and the obtained solid residue was dissolved again in a
139 smaller amount of 5 % HNO₃ to increase the trace element concentration. The resulting milky solution
140 was left to rest for 1 month to allow the insoluble residue to sediment out. The top clear portion of the
141 solution was then separated and analyzed by ICP-MS. Compositions of the MORB glasses and of the
142 solutions for reversed experiments are reported in Rustioni et al. (2019).

143 A solution with known composition was prepared in order to test various analytical approaches. Two
144 separate solutions were produced by dissolving CsOH and Na₂SiO₃ in distilled water in one case and

145 NaCl and KCl in in distilled water for the other solution. The final solution was then produced by mixing
146 the CsOH-Na₂SiO₃ solution with the NaCl-KCl solution to obtain the composition reported in Table 1.

147

148 **High pressure experiments**

149 In all experiments, a cylindrical Au or Pt capsule with 10 mm length, 5 mm external diameter and 4.6 mm
150 internal diameter was used. A 2 mm thick layer of diamond powder (10-20 μm grain size) was placed in
151 the central part of the capsule in between two layers of solid starting material. Fluid was either completely
152 added before the solid starting material, or it was added in several steps during the filling of the capsules.
153 In the second case, about 1/3 of the total fluid was added at the beginning, while the remaining fluid was
154 inserted after the diamond trap layer. This approach is particularly important when a fine-grained powder
155 is used, to prevent the solid starting material from being suspended and contaminating the diamond trap
156 layer during capsule preparation, which would cause an overestimation of solute content in the fluid phase
157 during LA-ICP-MS analysis after the experiments. About 1 mm of empty space was always left at the top
158 of the capsule to avoid fluid loss during the welding of the top lid. The weight of the capsule was always
159 checked before and after welding. Before high pressure experiments, the capsules were also left overnight
160 in an oven at 130 °C and weighed again to test whether complete sealing was achieved.

161 High pressure and temperature experiments were conducted in an end-loaded piston cylinder apparatus
162 using ½ inch MgO-NaCl assemblies with a stepped graphite furnace. Pressure was calculated from the oil
163 pressure on the hydraulic ram, using a 5 % friction correction, as calibrated by the quartz-coesite
164 transition and the density of synthetic fluid inclusions. Temperature was measured with a Pt/Pt-Rh (S-
165 type) thermocouple and monitored by a Eurotherm controller. The temperature was raised at constant
166 pressure after compression at a rate of 100 °C/min. Run durations varied depending on the complexity of
167 the system. For experiments on simple systems used in the solubility tests, the typical duration was 16-20
168 hours. In the eclogite-water ± NaCl system, experiment duration varied from 2 to 7 days. Most of the runs

169 were quenched by shutting off the power at constant pressure before starting the decompression. In a few
170 experiments conducted in the eclogite-water system, a cooling ramp of 100 °C/min was applied instead of
171 the temperature quench.

172 In the eclogite-water ± NaCl experiments at 4 GPa and 800 °C, some of the Au capsules appeared very
173 deformed and contained small holes after the experiments. The extent of deformation could be reduced by
174 pre-shrinking the capsule inside a hydrothermal vessel pressurized to 200 MPa before the piston cylinder
175 runs, in order to eliminate the empty space at the top of the capsules that was considered to be
176 mechanically weaker. However, this method did not particularly enhance the resistance of the capsule and
177 tiny holes were still observed after experiments. The problem was eventually solved by changing the
178 capsule material from gold to platinum and by slowly compressing and decompressing the sample over
179 16-20 hours at the beginning and the end of the experiments. Slow, continuous compression and
180 decompression was achieved using an automated hydraulic spindle press that continuously changed the
181 oil pressure on master ram and endload according to a pre-set program.

182 Another challenge in the eclogite-water experiments was to synthesize crystals (in particular omphacite)
183 large enough for LA-ICP-MS analysis. To overcome this problem, the initial fluid/solid starting material
184 ratio in the capsule was increased from ~ 0.3 to ~ 0.4. Moreover, temperature fluctuations of ± 30 °C
185 were applied in experiments to enhance grain growth by Ostwald ripening, i.e. the dissolution of smaller
186 crystals upon heating and the growth of larger crystals during cooling. Temperature cycling started after
187 an initial equilibration at constant temperature for ~ 36 hours to nucleate the mineral assemblage stable at
188 800 °C. The temperature cycling was stopped ~ 24 hours before quenching to let the system equilibrate
189 again. Ramps in temperature (from 770 to 830 °C and vice versa) lasted 2 hours each, with dwell times at
190 both temperatures of 2 hours. A single temperature cycle thus lasted 8 hours in total, see Figure 1.

191

192 **Analytical methods**

193 Several analytical approaches were tested, as described below. The best quality of data was obtained
194 when the fluid contained in the diamond trap was directly analyzed in frozen state by LA-ICP-MS
195 following a procedure similar to that described in Kessel et al. (2004). The capsules were cooled in liquid
196 nitrogen and then cut open longitudinally with a razor blade attached to an opening device. One half of
197 the frozen capsule was then quickly transferred to a LA-ICP-MS sample chamber equipped with a Peltier-
198 cooling element to keep the sample frozen during the entire measurement. Tests with H₂O-ethanol
199 mixtures revealed that the temperature within this sample chamber was ca. -30 °C. The LA-ICP-MS
200 measurements were performed with a 193 nm ArF GeolasPro laser ablation unit (Coherent, USA)
201 connected to an Elan DRC-e quadrupole ICP-MS unit (Perkin Elmer, Canada). The sample chamber was
202 flushed with He at a flow rate of 0.4 l/min, to which 5 ml/min H₂ was admixed on the way to the ICP-MS.
203 Measured isotopes included ⁷Li, ⁹Be, ¹¹B, ²³Na, ²⁵Mg, ²⁷Al, ³⁰Si, ³⁵Cl, ³⁹K, ⁴³Ca, ⁴⁵Sc, ⁴⁹Ti, ⁵⁷Fe, ⁸⁵Rb, ⁸⁸Sr,
204 ⁸⁹Y, ⁹³Nb, ¹³³Cs, ¹³⁷Ba, ¹³⁹La, ¹⁴⁰Ce, ¹⁴⁶Nd, ¹⁴⁷Sm, ¹⁵³Eu, ¹⁵⁷Gd, ¹⁶³Dy, ¹⁶⁷Er, ¹⁷²Yb, ¹⁷⁵Lu, ¹⁸¹Ta, ²⁰⁸Pb, ²³²Th,
205 and ²³⁸U, using a dwell time of 10 ms. The ICP-MS was tuned to a thorium oxide production rate of 0.05-
206 0.10 % and a rate of doubly-charged Ca ions of 0.15-0.25 % based on measurements on NIST SRM 610
207 glass (Jochum et al. 2011). The diamond trap layer was analyzed first by moving the laser beam at
208 constant velocity along a transect perpendicular to the diamond layer in order to locate and subsequently
209 avoid eventual contaminations at the border of the diamond trap. A second transect, parallel to the
210 diamond layer, was measured in the central, homogeneous part of the diamond trap. To obtain the best
211 average of fluid composition, a large laser spot size of 50-70 μm and a repetition rate of 7 Hz were used.
212 The signals resulting from each transect (a typical example is shown in Figure 2) were divided into 3-6
213 separate integration intervals, for which element concentrations were calculated. The average composition
214 of these intervals was considered to be representative of the fluid composition. The NIST SRM 610 glass
215 and a well-characterized, natural afghanite crystal (Seo et al. 2011) were used as external standards.
216 Cesium and/or chlorine were used as internal standards, as these elements are expected to partition
217 strongly into the fluid in all the systems investigated in the present study. Internal standard concentrations

218 used for calculation were corrected considering the dilution effect due to major element dissolution into
219 the fluid during high pressure and temperature experiments.

220 After analysis of the diamond trap of the eclogite-fluid partitioning experiments, the capsules were left to
221 evaporate at room temperature and subsequently they were impregnated in epoxy resin and polished to
222 expose minerals for LA-ICP-MS measurements. The largest suitable spot sizes to analyze single crystals
223 were typically in the range of 7-20 μm . Special care was taken during the garnet measurements to only
224 analyze inclusion-free rim portions and to avoid the natural garnet seeds, which showed distinctively
225 different composition. Averages obtained from measurements of 4 to 7 separate crystals within the
226 capsule were used to calculate the compositions of garnet, omphacite and rutile. Kyanite crystals were
227 also analyzed, but trace element concentrations were always below the detection limits and thus were
228 considered irrelevant for partitioning calculation. To calculate bulk fluid/eclogite partition coefficients,
229 first the fluid/mineral partition coefficients for each mineral were calculated, and then the results
230 normalized to a representative eclogitic composition of 59 % omphacite, 39 % garnet and 2 % rutile.

231

232 **RESULTS AND DISCUSSION**

233 **Test of various analytical approaches**

234 Simplified diamond trap experiments were carried out to understand which analytical approach provides
235 the most reliable data. Capsules were prepared following the procedure described above. Undoped
236 MORB glass was used as solid starting material, and an aqueous Na-Cl-Si-K-Cs solution of known
237 composition (see Table 1) was added to the capsules. Three experiments were conducted in a cold-seal
238 vessel at 200 MPa and room temperature for 1 hour in order to mechanically force the fluid into the pore
239 space between the solid materials and the diamond trap without changing its composition. The retrieved
240 capsules were weighed to check that no fluid loss or gain occurred during experiments. After these
241 experiments, three different procedures were used to analyze the diamond traps. One capsule was cut

242 open longitudinally and was allowed to evaporate at room conditions for three days (evaporation
243 approach). The second was frozen in liquid nitrogen, cut open, and then transferred in frozen state into a
244 Christ Alpha 2-4 LDplus freeze-drying apparatus with an ice condensation temperature of -85 °C, where
245 the aqueous liquid sublimated over the course of 2 hours (freeze-drying approach). In both the
246 evaporation and the freeze-drying approaches, after complete drying, one half of the capsule was
247 impregnated in epoxy and polished for further analysis. For the third capsule, the procedure described in
248 the “analytical methods” section was used (freezing chamber approach).

249 Results of these tests are shown in Figure 3 and Table 1, together with the original composition of the
250 fluid loaded into the capsule. Assuming that no major change in fluid composition occurred during the
251 experiments, the most accurate and precise method for analysis is clearly the freezing chamber approach.
252 The concentrations of Na, K, and Cs are reproduced within a relative deviation of 3.6, 14, and 4.2 %.
253 Only for silica, the measured concentration is 25 % below the expected value. This could, however,
254 reflect adsorption of silica on the surface of the glass powder in the charge. While the data obtained with
255 the freezing chamber are very stable and reproducible, both the evaporation and the freeze-drying method
256 give much more scattered results and even the averages sometimes deviate from the expected composition
257 by more than a factor of two (Table 1). Since none of the solute components in the fluid is expected to be
258 volatile near ambient temperature, the scatter is unlikely to be due to element loss during evaporation.
259 However, some redistribution of elements inside the diamond trap during evaporation could very well
260 explain the scatter of the data. Consistent with the test results described above, only the freezing chamber
261 approach was used to analyze the samples from high-pressure experiments that are discussed in the
262 following sections.

263

264 **Solubility measurements in known systems**

265 Several test experiments were carried out to measure mineral solubilities in water for simple, well-studied
266 systems, in order to compare the diamond trap method with data from literature. Results are shown in
267 Figure 4 and Table 2.

268 Two experiments (SC05 and SC06) were performed at 1 GPa and 800 °C to test quartz solubility in water.
269 This system is very well studied and there is generally a rather good agreement between various
270 experimental data sets (e.g. Anderson and Burnham 1965, Fournier and Potter 1982, Manning 1994). At
271 the conditions of the experiments, SiO₂ concentration in the fluid is expected to be 7 wt. % (Manning
272 1994). The solubility measured in experiment SC05 is 7.2 ± 0.5 wt. %, consistent with literature data. On
273 the other hand, experiment SC06 gave a significantly lower solubility of 4.2 ± 0.5 wt. %. The
274 experimental procedures for SC05 and SC06 were the same, also both diamond traps show relatively
275 homogeneous laser ablation signals along the analyzed transects, resulting in similar precision. Therefore,
276 the reason for the lower solubility obtained from experiment SC06 is not obvious. The slightly shorter run
277 duration of SC06 (16 hours) as compared to SC05 (18 hours) could have contributed to incomplete
278 attainment of equilibrium; however, the variation in the run durations is too small to account for the
279 observed differences in solubility.

280 The solubility of silica in the forsterite-enstatite-water system at 1 GPa and 800 °C was tested in
281 experiment SC02. The diamond trap approach yields well-reproducible data with an average of $0.94 \pm$
282 0.03 wt. % for the SiO₂ concentration in the fluid. However, this value is significantly below the silica
283 solubility determined by Newton and Manning (2002), who report a value of 1.77 wt. % SiO₂ at the same
284 conditions. A possible reason for the observed low solubility could be incomplete equilibration or perhaps
285 some error associated with the concentration of the Cs standard in the fluid. The run duration of 20 hours
286 is at the low end of those used by Newton and Manning (2002). However, in the latter study, a double
287 capsule technique was used in combination with single crystals, which should make attainment of
288 equilibrium more sluggish than in the present experiments. The high reproducibility in the diamond trap,
289 which reflects a homogeneous fluid and precipitate distribution in the capsule, is consistent with

290 equilibrium throughout the charge. Overall, the experiments in the quartz-H₂O and forsterite-enstatite-
291 H₂O systems indicate that silica concentrations in fluids can be measured with a precision of about 10 %
292 or better, but the accuracy of the measurements is likely lower, as they return the expected values only
293 within a factor of two or better.

294 Corundum solubility tests yielded data with both low precision and low accuracy. The average value for
295 Al₂O₃ concentration in the fluid for a diamond trap experiment (SC12) conducted at 2 GPa and 700 °C is
296 0.101 ± 0.009 wt. %. For these conditions, Tropper & Manning (2007) report a much lower corundum
297 solubility of 0.029 wt. %. The scatter in the measured concentrations in the diamond trap may be due to
298 inhomogeneous precipitation of solid materials either during the experiment or upon quench from high
299 temperature. Indeed, such effects are known from previous studies (e.g. Tropper and Manning 2007,
300 Antignano and Manning 2008). Corundum solubility increases strongly with temperature and therefore,
301 minute temperature gradients inside a capsule may cause the dissolution and re-precipitation of corundum
302 crystals throughout the charge. Images of such “vapor-transport crystals” are shown by Tropper and
303 Manning (2007). They are likely responsible for the anomalously high apparent solubilities observed in
304 experiment SC12 and for similar order-of-magnitude differences in corundum solubilities reported in
305 previous studies (e.g. Ragnasdottir and Walther 1985, Walther 1997).

306 Rutile solubility in water is known to be notoriously difficult to measure. Early single-crystal weight-loss
307 experiments in piston cylinder presses suggested very high solubilities up to 1.9 wt. % at 1 GPa and 1100
308 °C (Ayers and Watson 1993). These data were, however, very likely affected by dissolution and re-
309 precipitation effects in a temperature gradient. In later studies, Tropper and Manning (2005) and
310 Antignano and Manning (2008) carefully reduced temperature gradients inside the piston cylinder
311 experiments and obtained solubilities that were orders of magnitude lower. Direct visual observation of
312 rutile dissolution and re-precipitation in an externally-heated diamond cell yielded even lower solubilities
313 in the range of 10 to 25 ppm at 900 to 1050 °C and 1 to 2.5 GPa (Audétat and Keppeler 2005). As rutile
314 solubility may be strongly affected by temperature gradients, in experiment SC07 three separated

315 diamond traps were placed in the capsule to also test the temperature distribution. Therefore, in addition
316 to the diamond powder layer located at the center, one diamond trap was inserted at the bottom and one at
317 the top of the capsule, with two rutile layers dividing the three diamond layers. TiO₂ concentrations
318 measured in the fluid with this approach are very inhomogeneous, with no systematic difference observed
319 between the three diamond traps. As in previous studies, the measured concentrations are likely affected
320 by dissolution and precipitation in a temperature gradient along the entire capsule. This process also leads
321 to an overestimation of TiO₂ solubility, which at 2 GPa and 1000 °C is expected to be about 0.003 wt. %
322 (Audétat and Keppler 2005), while in our measurements it ranges between 0.017 and 0.042 wt. %. At face
323 value, these numbers would be more consistent with the rutile solubility model of Antignano and
324 Manning (2008), which predicts 0.026 wt. % TiO₂ under the run conditions. However, the scatter of the
325 data suggests that they are likely affected by some transport process in a thermal gradient.

326 Two experiments (SC03 and SC04) were conducted at 1.8 GPa and 800 °C in the albite-water system. At
327 these conditions a supercritical fluid should form (Shen and Keppler 1997), and therefore a single,
328 homogeneous fluid phase should fill the entire pore space in the capsule. The albite starting material was
329 thus directly mixed with diamond and the entire capsule was regarded as a single diamond trap for the
330 fluid. The measured fluid composition turned out to be homogeneous along the entire capsule for both
331 experiments. As the fluid/solid ratio loaded in the two capsules was the same, the expected concentrations
332 in the fluid for both runs are 35.9 wt. % SiO₂, 10.9 wt. % Al₂O₃, and 6.0 wt. % Na₂O. The expected SiO₂
333 concentrations are returned within 7 % relative or better in both experiments. In run SC03, Na₂O is
334 reproduced within 13 % relative, while in SC04, the Na₂O content is overestimated by 77 %, i.e. by
335 almost a factor of two. Since there is no obvious difference between experiments SC03 and SC04, this
336 result is in line with the observations made in the silica-H₂O and forsterite-enstatite-H₂O systems,
337 indicating that the intrinsic accuracy of the method is such that it reproduces the true concentrations
338 within a factor of two or better.

339 The measured Al_2O_3 concentrations in SC03 and SC04 are both less than half the expected value. This
340 may be caused by a fractionation process. To understand the origin of this problem, we filled a smaller
341 platinum capsule (4 mm high and 4 mm in diameter; sample AbTest) with a mixture of diamond and
342 albite powder in a ratio of about 9:1 plus added water in a similar fluid/solid ratio as in the experiments
343 SC03 and SC04. The capsule was compressed in a cold-seal vessel at 200 MPa without any heating and
344 then analyzed in frozen state in the same way as SC03 and SC04. The $\text{SiO}_2/\text{Al}_2\text{O}_3$ ratio obtained from this
345 test is 7.5, which is close to that obtained in SC03 and SC04, but significantly different from the
346 theoretical $\text{SiO}_2/\text{Al}_2\text{O}_3$ weight ratio of 3.54 in albite. In contrast, LA-ICP-MS analyses on a larger
347 fragment of albite using the same laser settings returned the correct $\text{SiO}_2/\text{Al}_2\text{O}_3$ ratio. Note that the frozen
348 diamond trap ablates in a far less controlled fashion than solids, resulting in deep trenches that are 2-5
349 times wider than the used beam diameter. The uncontrolled ablation likely causes serious fractionation
350 effects, particularly for refractory elements like Al. We thus believe that the low Al_2O_3 values represent
351 an analytical artifact.

352 Overall, the data presented here suggest that the analytical precision of the diamond trap technique is high
353 and that the accuracy is commonly within a factor of two or better, except in systems that are highly
354 susceptible to dissolution and re-precipitation of solid phases in minor temperature gradients, such as the
355 systems $\text{Al}_2\text{O}_3\text{-H}_2\text{O}$ and $\text{TiO}_2\text{-H}_2\text{O}$.

356

357 **Tests in partitioning experiments in the eclogite–water \pm NaCl system**

358 Compositions of fluid and minerals, and trace element fluid/eclogite partition coefficients obtained from
359 experiments in the eclogite–water \pm NaCl system using the methods described here were reported by
360 Rustioni et al. (2019). A frequent problem in such experiments is the difficulty to obtain crystals large
361 enough for trace element analysis. While in a crystal-melt system this can usually be solved by very slow
362 cooling and slow crystal growth from the melt, this is not possible for a system where crystals coexist

363 with an aqueous fluid only. However, we carried out some tests which suggest that periodic temperature
364 fluctuations can be used to enhance crystal growth through Ostwald ripening, i.e. the dissolution of
365 smaller crystals during heating and the growth of larger crystals during cooling. Figure 5 shows a
366 comparison between an eclogite synthesized in an experiment conducted at constant temperature (a) and
367 one obtained with ± 30 °C temperature fluctuations (b). Introducing temperature cycling effectively
368 enhanced omphacite and kyanite growth, while it did not particularly affect the size of garnet and rutile
369 crystals. Table 3 reports the average compositions of garnet and omphacite in two different experiments
370 (PC37 and PC38). Both experiments were conducted with pure water for a better comparison, but while in
371 PC38 the temperature was kept constant at 800 °C, in PC37 ± 30 °C temperature cycling was used. The
372 resulting compositions of both garnet and omphacite from the two experiments are very similar,
373 indicating that although temperature cycling enhanced crystal growth, it did not affect the composition of
374 minerals. This observation also applies for trace element compositions. A comparison between trace
375 element $D^{\text{fluid/eclogite}}$ between the same two experiments is shown in Figure 5c. Again, the measured
376 partition coefficients in PC37 and PC38 are the same within uncertainties. We therefore conclude that
377 temperature cycling can be a useful technique for enhancing crystal growth in fluid-mineral partitioning
378 experiments without compromising the validity of the measured partition coefficients (see also da Silva et
379 al. 2017). A necessary prerequisite for applying this method is, however, that the amplitude of cycling is
380 within the stability range of the phase assemblage of interest. While in a few experiments even at constant
381 temperature sufficiently large crystals were obtained to allow LA-ICP-MS analyses of all phases, in
382 particular the omphacite crystals were often too small for measuring trace element compositions. In such
383 cases, temperature cycling was very efficient for increasing crystal sizes.

384 The effect of different cooling rates on measured trace element concentrations was tested by comparing
385 experiment PC25, which was quenched from high temperature by shutting off the power resulting in a
386 rapid cooling within 10-15 seconds, to experiment PC27, which was cooled at a constant rate of 100
387 °C/minute. All other parameters in the experimental procedure of PC25 and PC27 were the same. Figure 6

388 shows that the two different cooling rates did not have major effects on the measured partition
389 coefficients for most of the trace elements.

390 In all experiments, LA-ICP-MS signals obtained from the analysis of frozen fluid in the diamond trap
391 were relatively constant in time for the measured isotopes (Figure 2). As the ablation was performed by
392 moving along transects perpendicular and parallel to the diamond layer, this reflects a generally
393 homogeneous distribution of elements inside the trap.

394 Kessel et al. (2005a) used a rocking multi anvil press to measure trace element partitioning in the
395 eclogite-fluid system. Schmidt and Ulmer (2004) suggested that such a device is necessary in order to
396 suppress the formation of extreme chemical zoning (and therefore disequilibrium) in fluid-bearing multi
397 anvil experiments. However, while this technology may indeed offer an advantage for multi anvil
398 experiments, where temperature gradients may be rather large, we did not observe any zonation or other
399 evidence for disequilibrium in our piston cylinder experiments. Figure 7 shows electron microprobe
400 measurements of garnets that were located in different areas of a capsule recovered from one piston
401 cylinder experiment. The composition is constant throughout the entire length of the recovered charge;
402 moreover, garnet and clinopyroxene appear to be homogeneously distributed, without obvious phase
403 segregation in parts of the capsule. Accordingly, equilibrium was likely achieved throughout the entire
404 charge. We therefore conclude that fluid/mineral partitioning experiments can be carried out with a
405 simple piston cylinder device up to about 5 GPa; the use of a rocking multi anvil in this pressure range is
406 not required.

407 Unlike for the mineral solubilities in simple model systems, it is not possible to test the accuracy of the
408 data obtained in eclogite-fluid partitioning experiments against independent measurements. However, it
409 was possible to check attainment of equilibrium between mineral and fluid phases by reversed
410 experiments. While in “forward” experiments all the trace elements were doped in the solid starting
411 material, in reversed experiments all the trace elements, except for Ti, were added by means of the fluid

412 phase and an undoped MORB was used. In general, we obtained good agreement between results from
413 forward and reversed experiments, typically within a factor of two, demonstrating attainment of
414 equilibrium in our experiments. Figure 8 shows the effect of Cl on the fluid/eclogite partition coefficient
415 of europium. The enhancement of Eu solubility with addition of chlorine is the same for forward and
416 reversed experiments.

417 In order to be able to measure trace element concentrations in both fluid and solid phases, it may be
418 necessary to dope the starting material with a relatively high concentration of trace elements. At the same
419 time, to measure meaningful partition coefficients, the concentration of trace elements must be low
420 enough to not exceed the boundaries of Henry's law behavior. Figure 8 includes results from experiments
421 conducted with different initial concentrations of europium. The fact that all experiments produce a single
422 trend implies that the Eu concentrations used in our experiments fulfill Henry's law. Similar data on
423 reversed experiments and variable trace element concentration for other trace elements are given by
424 Rustioni et al. (2019).

425 Taken together, the good agreement between forward and reversed experiments and the independence of
426 the measured partition coefficients on the bulk concentration of the trace elements suggests that in most
427 cases, the diamond trap method yields reliable fluid/eclogite partition coefficients within a factor of two.
428 However, the method can only be applied, if the system contains only one single mobile phase (fluid or
429 melt), as in the eclogite-water±NaCl system at 4 GPa and 800 °C (Kessel et al. 2005 b). In the presence of
430 both an aqueous fluid and a silicate melt, or in the presence of two coexisting fluids, distinguishing the
431 compositions of these phases by analyzing the diamond trap would be very difficult or impossible.

432

433

IMPLICATIONS

434 The systematic tests carried out in the course of this study show the potential and limitations of the
435 diamond trap technique for studying fluid compositions. In principle, the method is widely applicable for

436 both piston cylinder and multi anvil experiments, covering the entire pressure and temperature range of
437 the upper mantle. At least up to 5 GPa, partitioning and solubility experiments in fluid-bearing systems
438 may be carried out with conventional piston cylinder devices; the use of a rocking multi anvil is not
439 required in this pressure range. Laser ablation ICP-MS analyses of the fluid in the diamond trap should
440 always be carried out in frozen state. The method is particularly suitable for measuring partition
441 coefficients, which may vary by several orders of magnitude and thus do not require very high precision
442 or accuracy. However, particularly in chemically simple systems, measurements of mineral solubilities in
443 fluids using the single-crystal weight-loss techniques, or by direct observation in diamond anvil cells,
444 may yield more accurate results than the diamond trap method. A severe problem can be the dissolution
445 and re-precipitation of solid phases already during the high-pressure and high-temperature experiment,
446 which may lead to erroneously high fluid concentrations. Such effects are to be expected for phases like
447 corundum or rutile with solubilities that are highly temperature dependent, such that dissolution and re-
448 precipitation may occur as a result of minor temperature gradients.

449

450

ACKNOWLEDGEMENTS

451 We thank Marija Putak Juriček for helping with some of the experiments. Constructive reviews by Ronald
452 J. Bakker and an anonymous referee helped to improve the manuscript. This study was supported by the
453 DFG International Research Training Group “Deep Volatile Cycles”, (GRK 2156/1).

454

455

456

457

458

REFERENCES

459

460 Aerts, M., Hack, A.C., Reusser, E., and Ulmer, P. (2010) Assessment of the diamond-trap method for
461 studying high-pressure fluids and melts and an improved freezing stage design for laser ablation ICP-MS
462 analysis. *American Mineralogist*, 95, 1523-1526

463 Anderson, G.M. and Burnham, C.W. (1965) Solubility of quartz in supercritical water. *American Journal*
464 *of Science*, 263, 494-511

465 Antignano, A. and Manning, C.E. (2008) Rutile solubility in H₂O, H₂O-SiO₂, and H₂O-NaAlSi₃O₈ fluids
466 at 0.7-2.0 GPa and 700-1000 °C: Implications for mobility of nominally insoluble elements. *Chemical*
467 *Geology*, 255, 283-293.

468 Audétat, A. and Keppler, H. (2005) Solubility of rutile in subduction zone fluids, as determined by
469 experiments in the hydrothermal diamond anvil cell. *Earth and Planetary Science Letters*, 232, 393– 402.

470 Ayers, J.C. and Watson, E.B. (1993) Rutile solubility and mobility in supercritical aqueous fluids.
471 *Contributions to Mineralogy and Petrology*, 114, 321– 330.

472 Bali, E., Audetat, A., and Keppler, H. (2011) The mobility of U and Th in subduction zone fluids: an
473 indicator of oxygen fugacity and fluid salinity. *Contributions to Mineralogy and Petrology*, 161, 597–613.

474 Bali, E., Keppler, H., and Audetat, A. (2012) The mobility of W and Mo in subduction zone fluids and the
475 Mo-W-Th-U systematics of island arc magmas. *Earth and Planetary Science Letters*, 351, 195–207.

476 Bernini, D., Audetat, A., Dolejs, D., and Keppler, H (2013) Zircon solubility in aqueous fluids at high
477 temperatures and pressures. *Geochimica et Cosmochimica Acta*, 119, 178-187

- 478 da Silva, M.M., Holtz, F., and Namur, O (2017) Crystallization experiments in rhyolitic systems: The
479 effect of temperature cycling and starting material on crystal size distribution. *American Mineralogist*,
480 102, 2284-2294.
- 481 Fournier, R.O. and Potter, R.W. (1982) An equation correlating the solubility of quartz in water from 25
482 °C to 900 °C at pressures up to 10,000 bars. *Geochimica et Cosmochimica Acta*, 46, 1969-1973.
- 483 Jochum, K.P., Weis, U., Stoll, B., Kuzmin, D., Yang, Q.C., Raczek, I., Jacob, D.E., Stracke, A., Birbaum,
484 K., Frick, D.A., Gunther, D., and Enzweiler, J (2011) Determination of reference values for NIST SRM
485 610-617 glasses following ISO guidelines. *Geostandards and Geoanalytical Research*, 35, 397-429.
- 486 Johnson, M.C., and Plank, T. (1999) Dehydration and melting experiments constrain the fate of subducted
487 sediments. *Geochemistry Geophysics Geosystems*, 1, Article Number: 1007
- 488 Kawamoto, T., Yoshikawa, M., Kumagai, Y., Mirabueno, M.H.T., Okuno, M., and Kobayashi, T. (2013)
489 Mantle wedge infiltrated with saline fluids from dehydration and decarbonation of subducting slab.
490 *Proceedings of the National Academy of Sciences of the USA*, 110, 9663–9668.
- 491 Kelley, K.A., and Cottrell, E. (2009) Water and the oxidation state of subduction zone magmas. *Science*,
492 325, 605–607.
- 493 Keppler, H. (2017) Fluids and trace element transport in subduction zones. *American Mineralogist*, 102,
494 5–20.
- 495 Kessel, R., Ulmer, P., Pettke, T., Schmidt, M.W., and Thompson, A.B. (2004) A novel approach to
496 determine high-pressure high-temperature fluid and melt compositions using diamond-trap experiments.
497 *American Mineralogist*, 89, 1078-1086.
- 498 Kessel, R., Schmidt, M.W., Ulmer, P., and Pettke, T. (2005 a) Trace element signature of subduction-
499 zone fluids, melts and supercritical liquids at 120–180 km depth. *Nature*, 437, 724–727.

- 500 Kessel, R., Ulmer, P, Pettke T, Schmidt, M.W., and Thompson, A.B. (2005 b) The water–basalt system at
501 4 to 6 GPa: Phase relations and second critical endpoint in a K-free eclogite at 700 to 1400 °C. Earth and
502 Planetary Science Letters, 237, 873– 892.
- 503 Manning, C.E. (1994) The solubility of quartz in H₂O in the lower crust and upper mantle. Geochimica et
504 Cosmochimica Acta, 58, 4831–4839.
- 505 Manning, C.E. (2004) The chemistry of subduction zone fluids. Earth and Planetary Science Letters, 223,
506 1–16.
- 507 Newton, R.C., and Manning, C.E. (2002) Solubility of enstatite + forsterite in H₂O at deep crust/upper
508 mantle conditions: 4 to 15 kbar and 700 to 900°C. Geochimica et Cosmochimica Acta, 66, No. 23, 4165–
509 4176.
- 510 Potter, J.M., Pohl, D.C., and Rimstidt, J.D. (1987) Fluid flow systems for kinetic and solubility studies.
511 In: Hydrothermal Experimental Techniques (G.C. Ulmer, H.L. Barnes, eds.), John Wiley, 240-260.
- 512 Ragnarsdottir, K.V., and Walther, J.V. (1985) Experimental determination of corundum solubilities in
513 pure water between 400–700 °C and 1–3 kbar. Geochimica et Cosmochimica Acta, 49, 2109–2115.
- 514 Rustioni, G., Audétat, A., and Keppler, H. (2019) Experimental evidence for fluid-induced melting in
515 subduction zones. Geochemical Perspectives Letters, 11, 49-54.
- 516 Ryabchikov, I.D., and Boettcher, A.L. (1980) Experimental evidence at high pressure for potassic
517 metasomatism in the mantle of the Earth. American Mineralogist, 65, 915-919.
- 518 Ryabchikov, I.D., Orlova, G.P., Kalenchuk, G.Y., Ganeyev, I.I., Udovkina, N.G., and Nosik, L.P. (1989)
519 Reactions of spinel lherzolite with H₂O-CO₂ fluids at 20 kbar and 900 °C. Geochemistry International, 26,
520 56–62.

- 521 Schmidt, M.W., and Ulmer, P. (2004) A rocking multianvil: elimination of chemical segregation in fluid-
522 saturated high-pressure experiments. *Geochimica et Cosmochimica Acta*, 68, 1889-1899.
- 523 Shen, A.H. and Keppler, H. (1997) Direct observation of complete miscibility the albite-H₂O system.
524 *Nature*, 385, 710-712.
- 525 Seo, J.H., Guillong, M., Aerts, M., Zajacz, Z., and Heinrich, C.A. (2011) Microanalysis of S, Cl, and Br
526 in fluid inclusions by LA-ICP-MS. *Chemical Geology*, 284, 35-44.
- 527 Stalder, R., Foley, S.F., Brey, G.P., and Horn, I. (1998) Mineral aqueous fluid partitioning of trace
528 elements at 900–1200 °C and 3.0–5.7 GPa: New experimental data for garnet, clinopyroxene, and rutile,
529 and implications for mantle metasomatism.
- 530 Tatsumi, Y. (1989) Migration of fluid phases and genesis of basalt magmas in subduction zones. *Journal*
531 *of Geophysical Research*, 94, 4697–4707.
- 532 Tropper, P. and Manning, C.E. (2005) Very low solubility of rutile in H₂O at high pressure and
533 temperature, and its implications for Ti mobility in subduction zones. *American Mineralogist*, 90, 502-
534 505.
- 535 Tropper, P., and Manning, C.E. (2007) The solubility of corundum in H₂O at high pressure and
536 temperature and its implications for Al mobility in the deep crust and upper mantle. *Chemical Geology*,
537 240, 54–60.
- 538 Tsay, A., Zajacz, Z., and Sanchez-Valle, C. (2014) Efficient mobilization and fractionation of rare-earth
539 elements by aqueous fluids upon slab dehydration. *Earth and Planetary Science Letters*, 398, 101–112.
- 540 Walther, J.V. (1997) Experimental determination and interpretation of the solubility of corundum in H₂O
541 between 350 and 600 °C from 0.5 to 2.2 kbar. *Geochimica et Cosmochimica Acta*, 61, 4955–4964.

542 Weiss, Y., McNeill, J., Pearson, D.G., Nowell, G.M., and Ottley, C.J. (2015) Highly saline fluids from a
543 subducting slab as the source for fluid-rich diamonds. *Nature*, 524, 339–342.

544 Wilke, M., Schmidt, C., Dubrail, J., Appel, K., Borchert, M., Kвашнина, K., and Manning, C.E. (2012)
545 Zircon solubility and zirconium complexation in $\text{H}_2\text{O}+\text{Na}_2\text{O}+\text{SiO}_2\pm\text{Al}_2\text{O}_3$ fluids at high pressure and
546 temperature. *Earth and Planetary Science Letters*, 349, 15–25.

547 Zarei, A., Klumbach, S., and Keppler, H. (2018) The relative Raman scattering cross sections of H_2O and
548 D_2O , with implications for in situ studies of isotope fractionation. *ACS Earth and Space Chemistry*, 2,
549 925–934.

550

551

Table 1. Tests of different analytical approaches

| Analytical approach | Initial fluid composition | Freeze-drying | Evaporation | Freezing chamber |
|--------------------------|---------------------------|---------------|-------------|------------------|
| Na ₂ O (wt.%) | 7.74 | 2.5 (7) | 5.6 (3) | 8.02 (6) |
| SiO ₂ (wt.%) | 3.12 | 7 (4) | 6 (2) | 2.35 (9) |
| Cl (wt.%)* | 7.62 | 7.62 | 7.62 | 7.62 |
| K ₂ O (wt.%) | 2.69 | 1.3 (2) | 3.7 (3) | 2.30 (4) |
| Cs (ppm) | 120 | 110 (20) | 148 (19) | 115 (4) |

One standard deviation is reported in parentheses in terms of the least digit cited

*Cl concentration in the fluid is used as internal standard for calculations

552

553

Table 2. Tests of mineral solubilities in known systems

| Experiment | Type | P (GPa) | T (°C) | Duration (h) | SiO ₂ | Al ₂ O ₃ | Na ₂ O | TiO ₂ |
|---------------|----------------------|---------|--------|--------------|------------------|--------------------------------|-------------------|------------------|
| SC05 | Quartz | 1 | 800 | 18 | 7.2 (5) | | | |
| SC06 | | | | 16 | 4.2 (5) | | | |
| SC02 | Forsterite-enstatite | 1 | 800 | 20 | 0.94 (3) | | | |
| SC12 | Corundum | 2 | 700 | 19 | | 0.101 (9) | | |
| SC07 (top) | | | | | | | | 0.023 (2) |
| SC07 (middle) | Rutile | 2 | 1000 | 18 | | | | 0.034 (1) |
| SC07 (bottom) | | | | | | | | 0.028 (6) |
| SC03 | Albite-water | 1.8 | 800 | 16 | 38.3 (7) | 4.9 (2) | 6.8 (3) | |
| SC04 | supercritical fluid | | | 16 | 37.0 (6) | 3.0 (2) | 10.6 (3) | |

One standard deviation is reported in parentheses in terms of the least digit cited

Concentrations are expressed as wt. % in the fluid phase

554

Table 3. Effect of temperature cycling on mineral compositions in the eclogite-H₂O system at 4 GPa and 800 °C

| Mineral | T cycling | SiO ₂ | TiO ₂ | Al ₂ O ₃ | MgO | CaO | FeO | Na ₂ O |
|-----------|-----------|------------------|------------------|--------------------------------|---------|----------|----------|-------------------|
| Garnet | No | 46.1 (12) | 0.67 (2) | 19.0 (9) | 7.5 (2) | 9.2 (7) | 17.5 (4) | 0.16 (5) |
| | Yes | 46.3 (4) | 0.71 (7) | 19.2 (4) | 8.1 (4) | 8.3 (4) | 17.4 (2) | 0.32 (4) |
| Omphacite | No | 59.3 (4) | 0.55 (4) | 14.2 (5) | 7.5 (2) | 13.4 (1) | 5.1 (3) | 6.73 (1) |
| | Yes | 61.4 (7) | 0.45 (4) | 14.6 (7) | 7.3 (1) | 11.8 (4) | 4.5 (4) | 6.88 (25) |

One standard deviation is reported in parentheses in terms of the least digit cited

Concentrations are expressed as wt. %.

555

556

557 **Figure captions**

558

559 **Figure 1.** Example of temperature profile in a typical eclogite-water system experiment in which ± 30 °C
560 temperature cycling was applied. On the left the entire experiment duration is shown. On the right is the
561 detail of a single temperature cycle with a total duration of 8 hours.

562 **Figure 2.** Representative LA-ICP-MS signal collected from the frozen fluid contained in the diamond
563 trap while moving along a transect parallel to the diamond layer from experiment PC39 conducted in the
564 eclogite-water system at 800 °C and 4 GPa. The fluid contained approximately 7 wt. % of Cl, 6 wt. % of
565 Na₂O, 27 wt. % of SiO₂, 1 wt. % Al₂O₃, 370 ppm of Ti and 6300 ppm of Cs.

566 **Figure 3.** Comparison between measurements of fluid compositions performed using three different
567 methods: “evaporation” (green triangles), “freeze drying” (red diamonds) and “freezing chamber” (blue
568 circles), as described in the text. The initial fluid composition is shown as a grey line.

569 **Figure 4.** Results of experiments to test mineral solubilities in known systems. Each graph gives the
570 results of a single experiment, and each point represents the integration of a segment of the laser ablation
571 transects performed on the diamond trap portions of the capsule. Expected concentrations in the fluid
572 from the literature are shown as a grey line. The data for quartz (experiment SC05) are from Manning
573 (1994), for forsterite-enstatite (SC02) from Newton and Manning (2002), for corundum (SC12) from
574 Tropper and Manning (2007), and for rutile (SC07) from Audétat and Keppler (2005). For the albite-H₂O
575 system (SC03), the P, T conditions are beyond the critical curve (Shen and Keppler 1997) and therefore
576 the measured composition should equal the bulk composition of the charge.

577 **Figure 5.** Comparison of experimental results in the eclogite–fluid system at 4 GPa and 800 °C
578 conducted with and without temperature fluctuation. (a) Eclogite synthesized in an experiment run at
579 constant temperature. (b) Eclogite synthesized in an experiment where ± 30 °C cycling was used. (c)

580 Comparison of trace element fluid/eclogite partition coefficient measured in two experiments conducted
581 at 4 GPa with pure water, one at a steady temperature of 800 °C and the other with temperature cycling.
582 Error bars correspond to one standard deviation.

583 **Figure 6.** Comparison of fluid/eclogite partition coefficients obtained from an experiment that was
584 rapidly quenched from high temperature, versus one that was cooled down at a rate of 100 °C/minute. In
585 general, variations in cooling rate were found to have little effect on the measured fluid compositions.
586 Error bars correspond to one standard deviation.

587 **Figure 7.** Garnet compositions measured along a single capsule from an experiment in the eclogite-fluid
588 system at 4 GPa and 800 °C. Red diamonds are iron, yellow triangles aluminium, blue squares calcium
589 and green circles magnesium oxides.

590 **Figure 8.** Effect of the amount of chlorine dissolved in fluid on the fluid/eclogite partition coefficient of
591 europium. Green diamonds represent data obtained from forward experiments. Red circles are data
592 obtained from reversed experiments. Different shades of color represent different initial concentration of
593 trace elements in the solid starting material (green diamonds) or in the initial fluid (red circles) used in
594 experiments. Error bars correspond to one standard deviation.

Figure 1

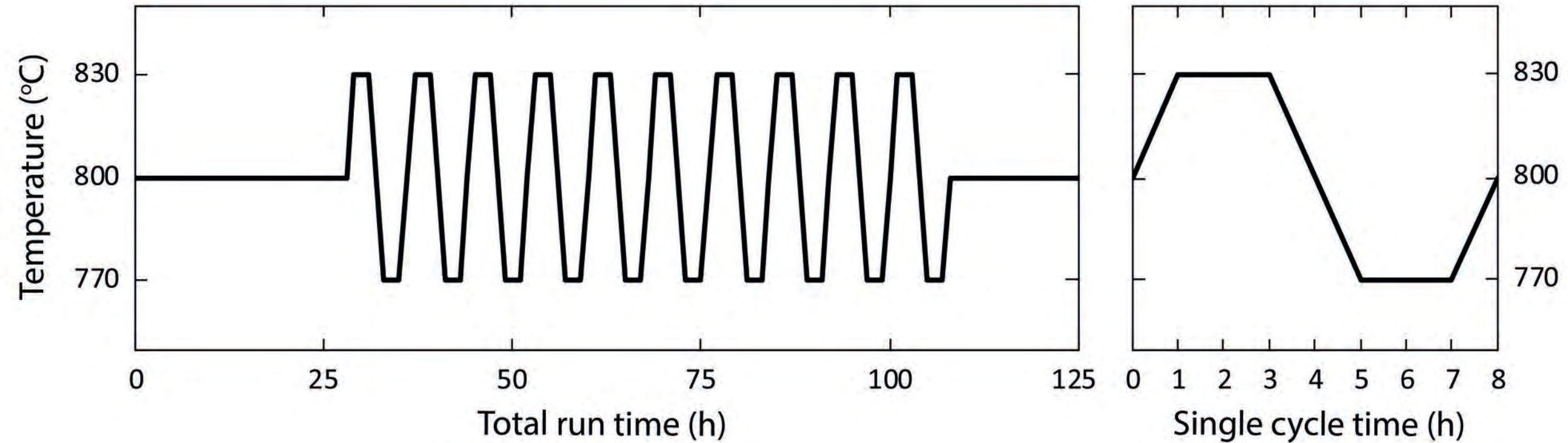


Figure 2

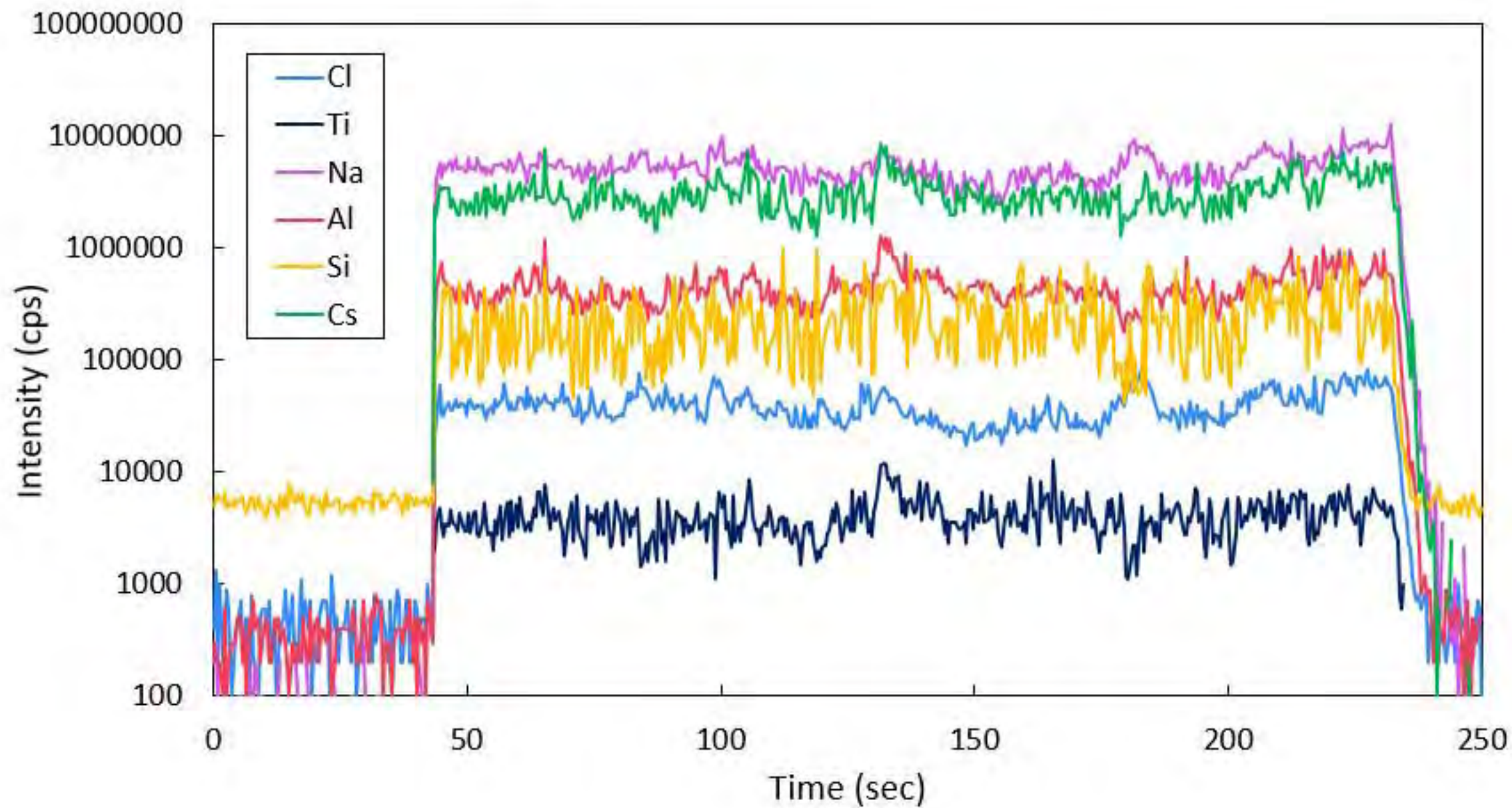


Figure 3

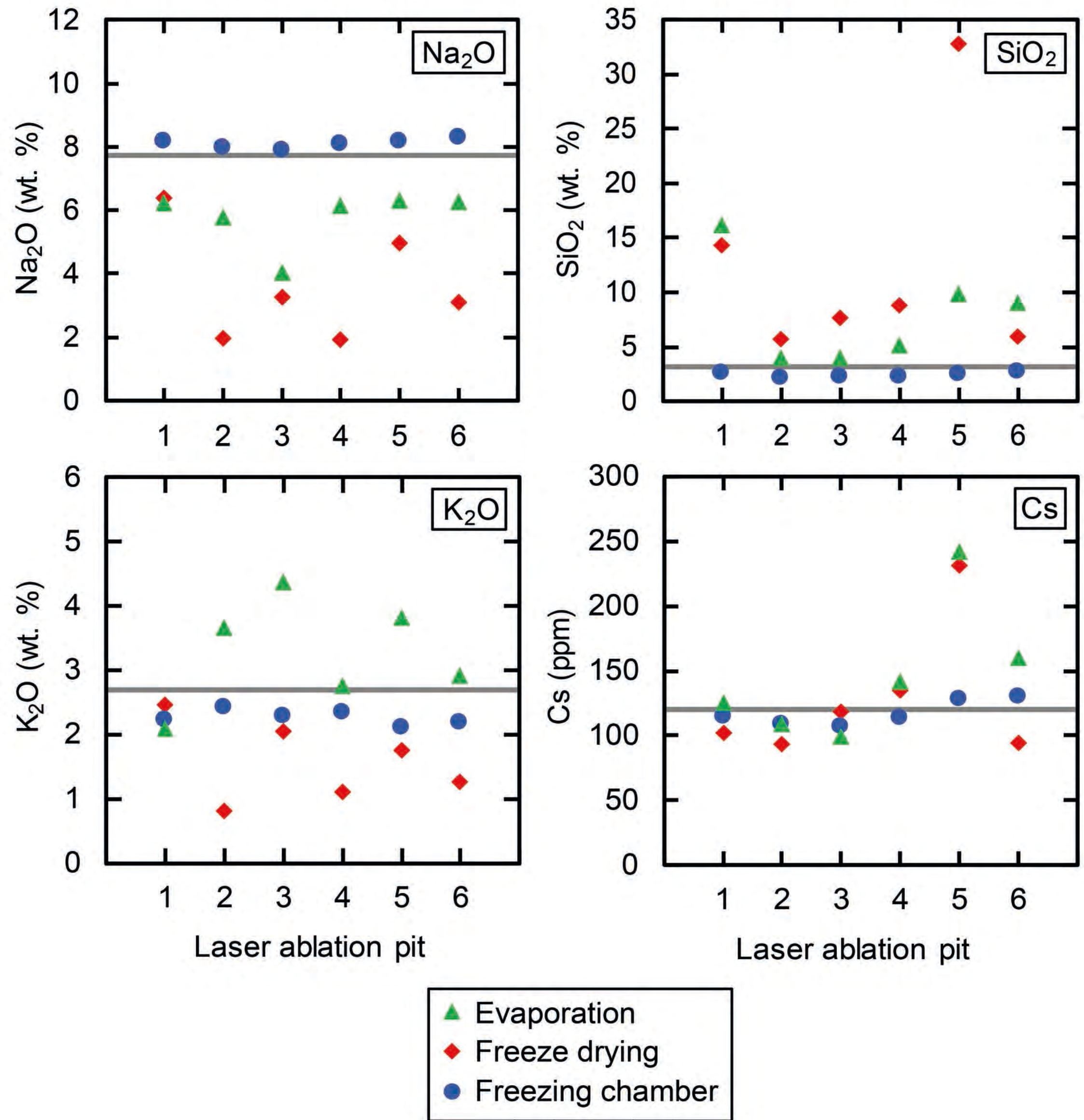


Figure 4

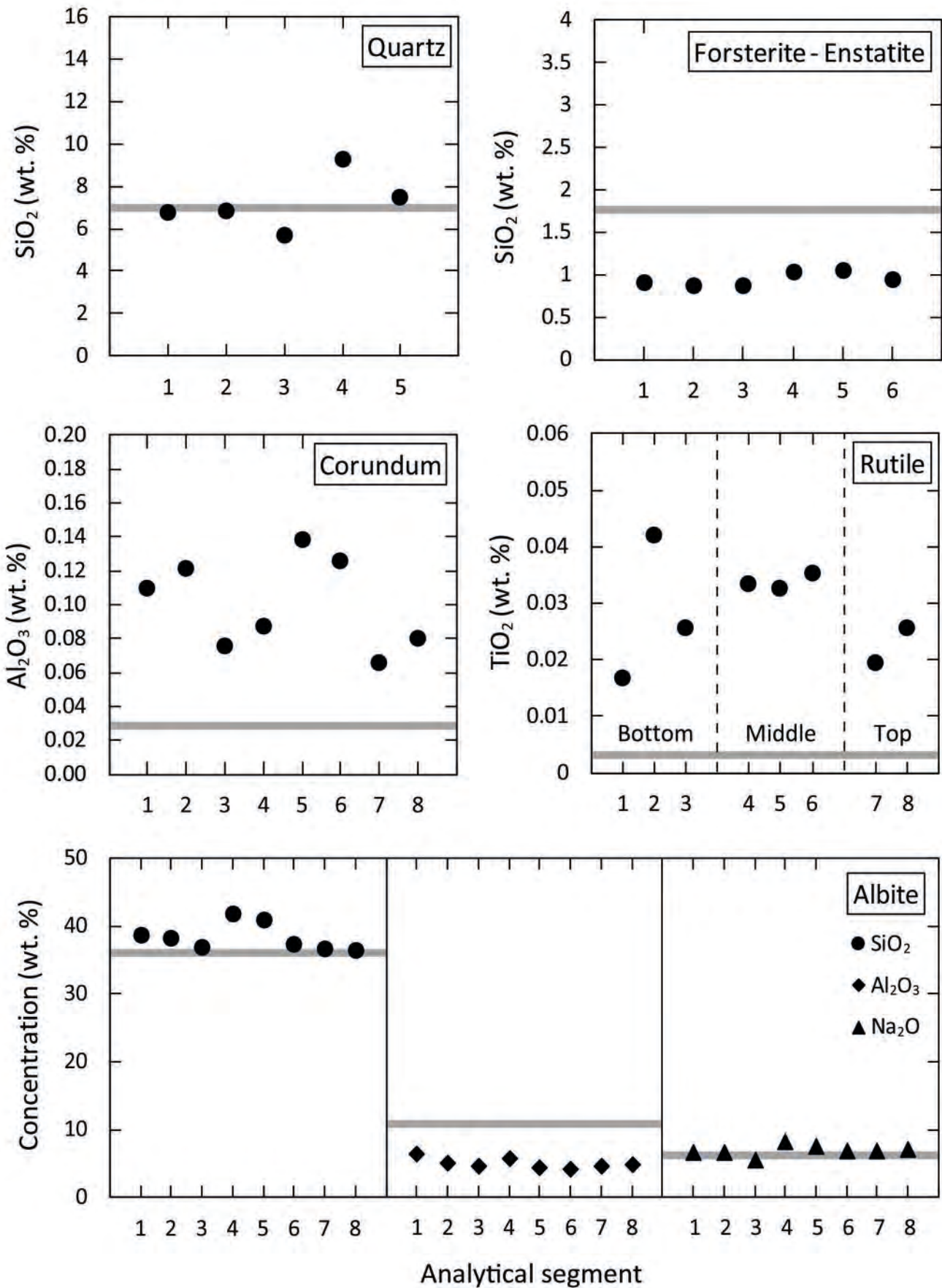


Figure 5

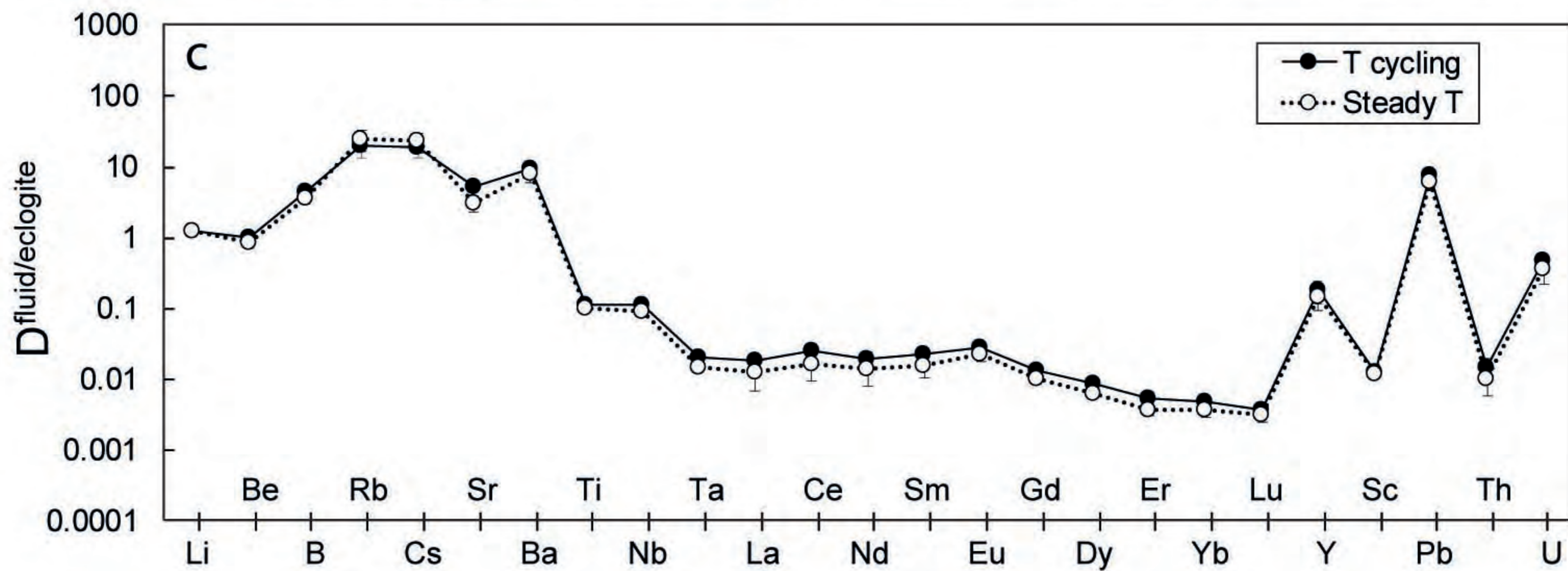
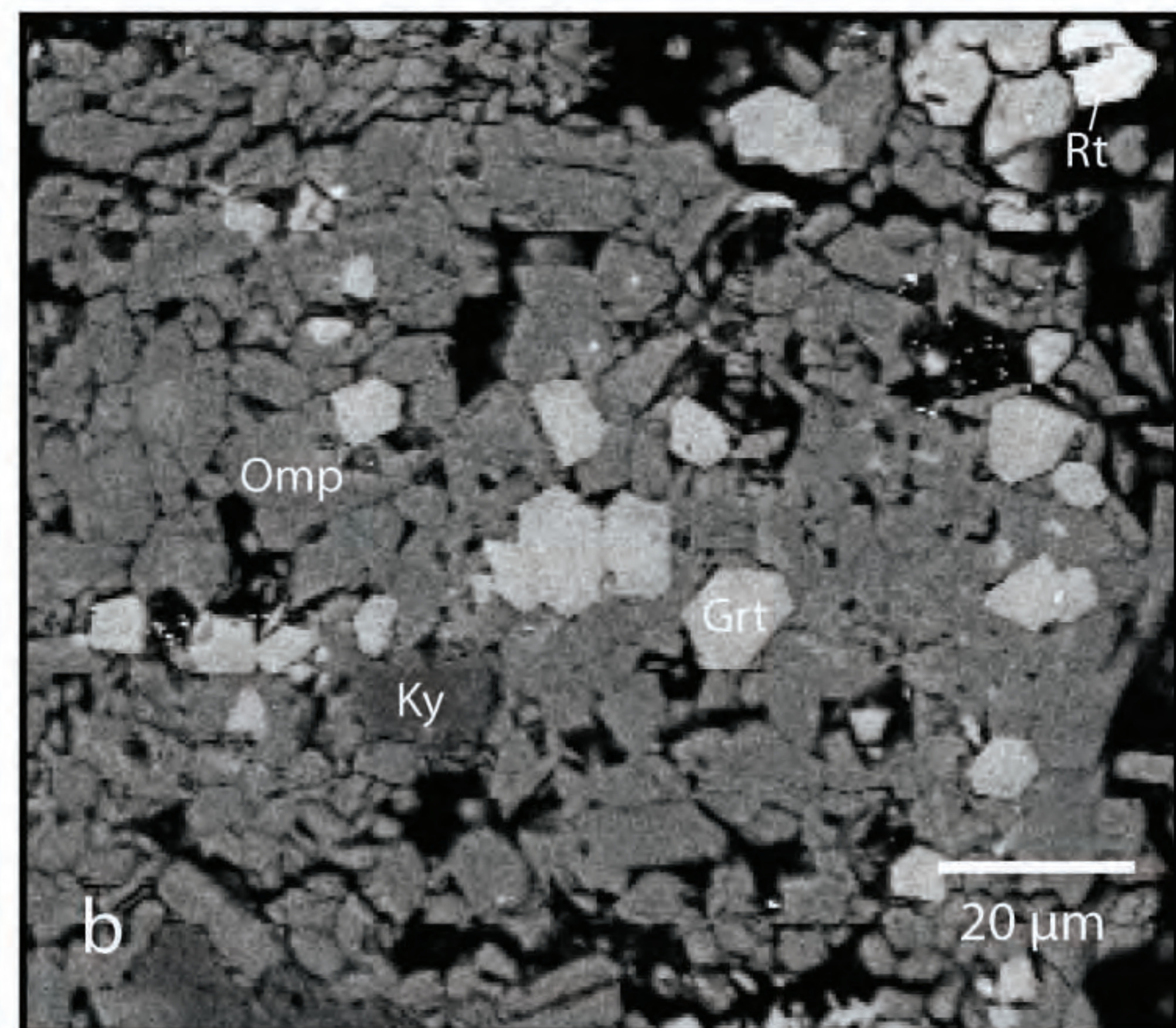
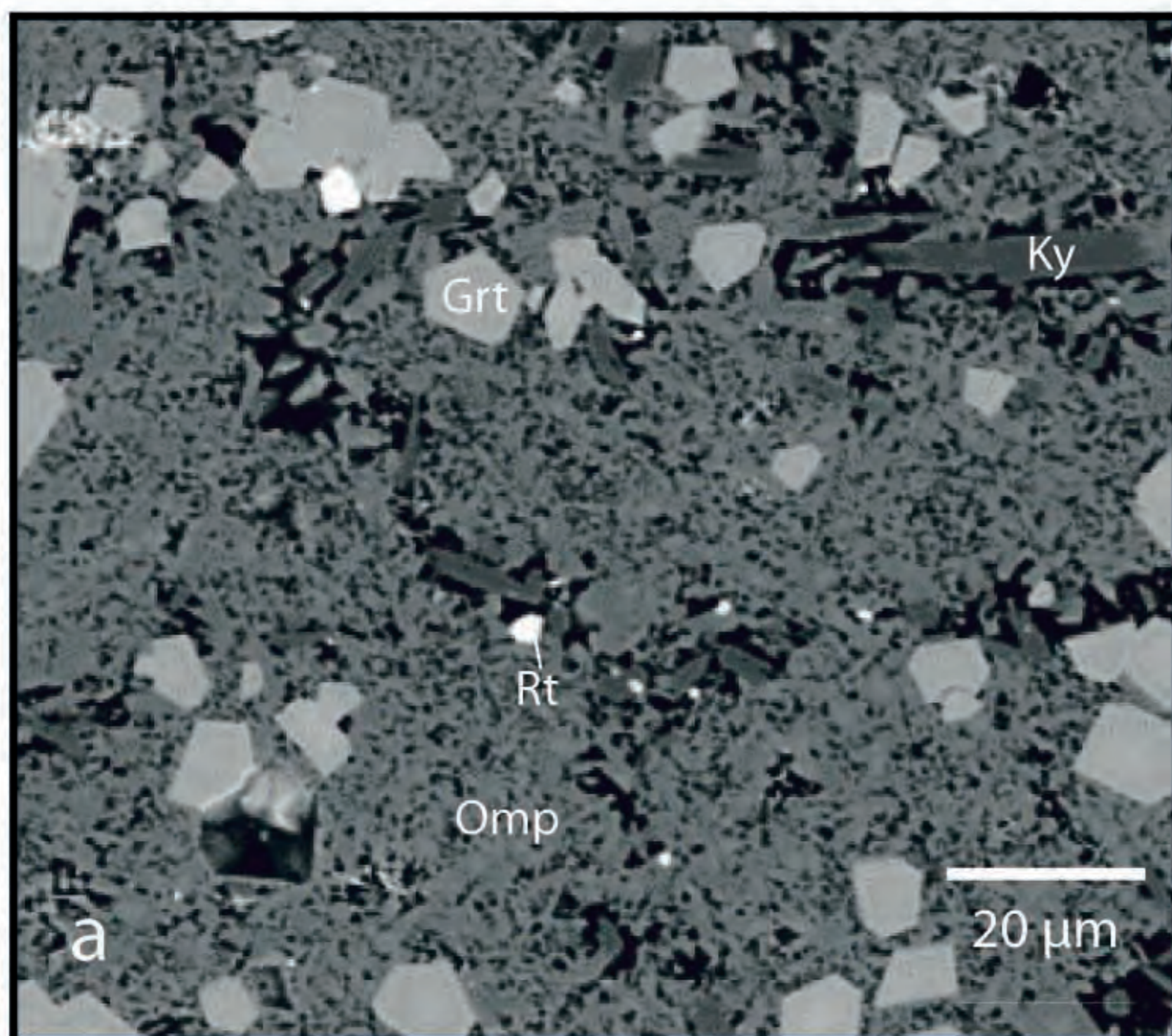


Figure 6

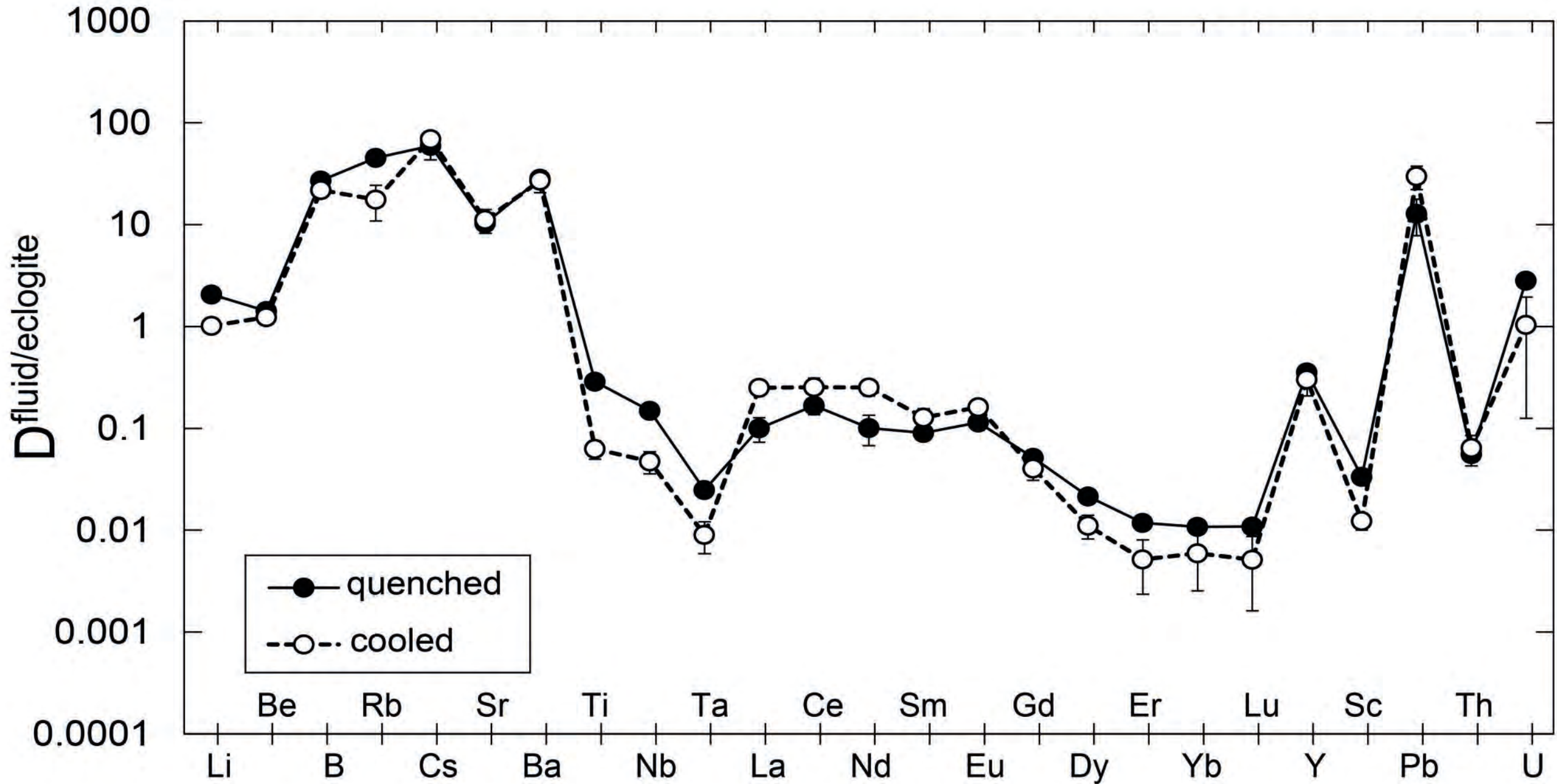


Figure 7

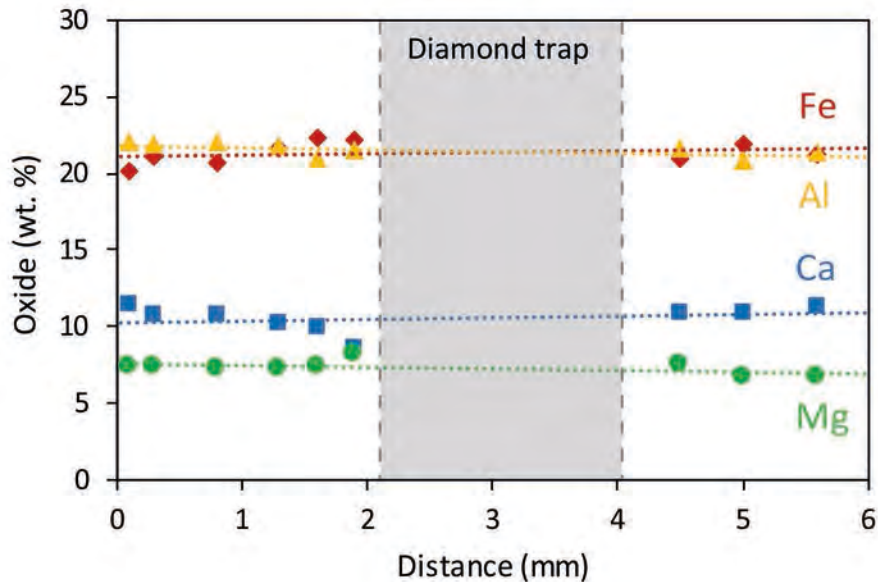


Figure 8

